

1 **COUPLING MEMBRANE SEPARATION AND PHOTOCATALYTIC OXIDATION**
2 **PROCESSES FOR THE DEGRADATION OF PHARMACEUTICAL POLLUTANTS**

3
4 **F. Martínez^{1,*}, M. J. López-Muñoz¹, J. Aguado¹, J.A. Melero¹, J. Arsuaga², A. Sotto²,**
5 **R. Molina¹, Y. Segura¹, M. I. Pariente¹, A. Revilla¹, L. Cerro¹, G. Carenas¹**

6
7 ¹Department of Chemical and Environmental Technology,

8 ²Department of Chemical and Energy Technology,

9 ESCET, Universidad Rey Juan Carlos, c/ Tulipán s/n, 28933 Móstoles, Madrid, Spain

10
11
12
13
14 Published on :

15 WaterResearch 47 (2013) 5647 – 5658

16 doi : <http://dx.doi.org/10.1016/j.watres.2013.06.045>

17

18 **Abstract**

19 The coupling of membrane separation and photocatalytic oxidation has been studied for the removal of
20 pharmaceutical pollutants. The retention properties of two different membranes (nanofiltration and
21 reverse osmosis) were assessed. Comparable selectivity on the separation of pharmaceuticals were
22 observed for both membranes, obtaining a permeate stream with concentrations of each pharmaceutical
23 below 0.5 mg/L and a rejected flux highly concentrated (in the range of 16-25 mg/L and 18-32 mg/L of
24 each pharmaceutical for NF-90 and BW-30 membranes, respectively), when an initial stream of six
25 pharmaceuticals was feeding to the membrane system (10 mg/L of each pharmaceutical). The abatement
26 of concentrated pharmaceuticals of the rejected stream was evaluated by means of heterogeneous
27 photocatalytic oxidation using TiO₂ and Fe₂O₃/SBA-15 in presence of hydrogen peroxide as photo-
28 Fenton system. Both photocatalytic treatments showed remarkable removals of pharmaceutical
29 compounds, achieving values between 80 and 100 %. The nicotine was the most refractory pollutant of all
30 the studied pharmaceuticals. Photo-Fenton treatment seems to be more effective than TiO₂ photocatalysis,
31 as high mineralization degree and increased nicotine removal were attested. This work can be considered
32 an interesting approach of coupling membrane separation and heterogeneous photocatalytic technologies
33 for the successful abatement of pharmaceutical compounds in effluents of wastewater treatment plants.

34 **Keywords:**

35 pharmaceutical pollutants, nanofiltration, reverse osmosis, photocatalysis, photo-Fenton

36 * **Corresponding author. Tel.: 91 4887182; Fax: 914887068.**

37 **e-mail address: fernando.castillejo@urjc.es.**

38

39 **1. Introduction**

40

41 Pharmaceuticals constitute a large group of medicinal human and veterinary compounds with a high
42 consumption worldwide. As pharmaceuticals are designed to increase their potency, bioavailability and
43 degradation resistance, they became persistent organic compounds in the environment (Xu et al., 2007).
44 Moreover these chemicals are not currently regulated by water-quality laws, which make them emerging
45 pollutants (Farré et al., 2008).

46 Although, the presence of these compounds in the environment corresponds to low concentration levels,
47 its continuous input from wastewater treatment plants or direct discharge to natural riverbeds may
48 represent a long-term potential threat for the aquatic and terrestrial ecosystems. Several authors have
49 reported that the health and environmental risks are not only associated with the impact of the bioactive
50 metabolites generated from the metabolic conversion of pharmaceutically active compounds (PhACs), but
51 also with plausible synergetic effects of the mixture of various bioactive metabolites in addition to other
52 micropollutants (Farré et al., 2008). Therefore, the pharmacologically valuable properties of
53 bioavailability and degradation resistance happen to be hazardous as they become unwelcomed exposures
54 of humans and the environment to bioactive anthropogenic compounds.

55 Several reports have reported a huge variety of PhACs and bioactive metabolites in influents and effluents
56 of wastewater treatment plants (WWTPs), rivers and drinking waters: antibiotics, analgesics,
57 antiepileptic, anti-rheumatics, beta blockers, chemotherapeutics and steroid hormones (Al-Rifai et al.,
58 2007; Gómez et al., 2007; Santos et al., 2010). Particularly in Spain, several studies on the efficacy of
59 WWTPs for the removal of PhACs have been performed with very sensitive analytical methods,
60 confirming the occurrence of high amounts of a variety of PhACs and subproducts in surface waters in
61 concentrations ranging from nano to micro grams per liter (Gros et al., 2007; Gomez et al., 2007;
62 Martinez-Bueno et al., 2007). The removal rates of PhACs in current WWTPs are, in general, around 40-
63 60% (Clara et al., 2005; Miegé et al., 2009). Therefore, it makes necessary the implementation of efficient
64 technologies in the wastewater treatment plants for the elimination of these refractory pharmaceuticals
65 residues prior to entering into the aquatic environment.

66 High pressure driven membrane processes as nanofiltration (NF) and reverse osmosis (RO) have appeared
67 as useful options to remove a wide range of organic contaminants in terms of solute rejection (Braeken et
68 al., 2006; Bousse et al., 2008; Lopez-Muñoz et al., 2009). Thus, numerous works have been focused on

69 the study of the main transport mechanisms of PhACs through commercially available NF/RO
70 membranes (Nghiem et al., 2005; Ozaki et al., 2008; Verliefde et al., 2009; Simon et al., 2009). Rejection
71 of pharmaceuticals by these membranes is really complex as consequence of the large number of
72 variables involved in the separation mechanisms. This parameter is influenced by the physic-chemical
73 properties of the solute (molecular weight, charge, hydrophobicity, dipole moment, and acid-base
74 character), the membrane properties (surface hydrophobicity and charge, pore size and water
75 permeability), the solution chemistry (ionic environment, pH and solute concentration) and the
76 operational conditions (temperature, trans-membrane pressure and cross-flow velocity). The application
77 of NF or RO separation processes can be very useful for the generation of a permeated stream of very
78 high quality, but a secondary stream with a concentrated solution of the retentate pollutants would be also
79 produced, requiring an additional treatment.

80 In order to sort out the final removal of pharmaceutical contaminants, the treatment of the retentate stream
81 by means of advanced oxidation processes (AOPs) can be taken into account. (Klavarioti et al., 2009).
82 Among them, AOPs based on UV irradiation such as heterogeneous photo-catalysis using TiO_2 or photo-
83 Fenton processes based on iron-containing catalysts in presence of H_2O_2 are considered of great potential.
84 Moreover, benefits in terms of disinfection can be accomplished. The photolysis (alone or combined with
85 an oxidant, such as H_2O_2) and heterogeneous photocatalysis with TiO_2 have been widely used for the
86 treatment of pharmaceuticals in aqueous solutions (Baran et al., 2006; Yang et al., 2008). For the
87 heterogeneous TiO_2 photocatalysis, an important effort has paid attention to the integration of
88 photocatalytic reactors with membrane cells that enable the separation and recirculation of TiO_2 catalysts
89 to the photoreactor. Thus, an increase in the overall performance of the process by the double effect of the
90 photocatalytic oxidation and the effective rejection of non-converted contaminants can be obtained. This
91 strategy has been found in literature for the treatment of different pollutants such as dyes (Grzechulska-
92 Damsz et al., 2009; Mozia et al., 2010) or even some pharmaceuticals (Molinari et al., 2006). In the case
93 of the photo-Fenton process, most of the studies have been focused on the application of the
94 homogeneous Fenton reagent based on the dissolution of iron salts in presence of hydrogen peroxide
95 (Perez-Estrada et al., 2005; Shemer et al., 2006; Klammerth et al., 2010). However, the application of new
96 heterogeneous photo-Fenton catalytic systems based on the immobilization of iron species over a solid
97 silica matrix, have offered promising results, avoiding the recovering of the iron ions from final effluent

98 and the restricted working pHs (2-3) that are necessary in homogeneous photo-Fenton systems
99 (Rodriguez-Gil et al., 2010; Molina et al., 2012).

100 The aim of this work is dealing with the application of membrane separation and heterogeneous
101 photocatalytic oxidation processes for the treatment of aqueous solutions containing pharmaceutical
102 pollutants. In this coupled system, two different membranes, one of nanofiltration and another of reverse
103 osmosis, were evaluated as selective barriers for the retention of pharmaceutical compounds.
104 Additionally, the efficiency of heterogeneous photocatalytic methods using the semiconductor Degussa P-
105 25 TiO₂ and hematite iron oxide supported over a mesoporous silica support (Fe₂O₃/SBA-15) was
106 assessed for the treatment of the resultant retentate stream.

107

108

109 **2. Materials and methods**

110

111 **2.1. Pharmaceuticals**

112 Six pharmaceuticals representative of different families of drugs were selected as model pollutants for the
113 assessment of separation/oxidation combined processes: sulfamethoxazole (SMX, antibiotic), diclofenac
114 sodium (DCF, anti-inflammatory), hydrochlorothiazide (HCT, diuretic, drug to treat hypertension), 4-
115 acetamidoantipyrine (4AAA, antipyretic), nicotine (NCT, stimulant) and ranitidine hydrochloride (RNT,
116 histamine H₂-receptor antagonist that inhibits stomach acid). They have been usually found in the
117 influents and effluents of wastewater treatment plants being hardly affected by the conventional treatment
118 processes (Gros et al., 2010). All of them were provided by Sharlab, with purity higher than 99 %.

119 Table 1 summarizes some physico-chemical properties of the selected pharmaceutical compounds. As it
120 can be seen, they all have rather similar molecular weights, except nicotine, but their hydrophobicity,
121 expressed as logarithm of octanol-water partition coefficient ($\log K_{ow}$) and the ionization balance
122 determined by the acid dissociation constant (pK_a) show a wide range of values. These features related to
123 hydrophobic and ionic interactions are usually of particular influence on the selective rejection of the
124 pollutants over the membrane surface.

125 Stock solutions of 20 L with 10 mgL⁻¹ of each pharmaceutical compound were prepared by simultaneous
126 dissolution of each solute in deionised Milli-Q water. The resultant combined mass concentration of the
127 stock solution was of ca. 60 mgL⁻¹ with a pH of ca. 7

128 Table 1

129

130 2.2. *Description of the separation/oxidation coupling system*

131 A coupling system of membrane separation and photocatalytic oxidation has been evaluated for the
132 removal of pharmaceuticals in wastewaters. The aqueous solution containing pharmaceuticals is fed to the
133 membrane unit, obtaining a permeate free of pollutants and a rejected flux with high concentration of
134 pharmaceuticals. Subsequently, the rejected stream was treated by photocatalytic systems. Two different
135 photo-catalytic technologies have been studied, one of them using TiO₂ as heterogeneous catalyst and
136 another one using Fe₂O₃/SBA-15 and hydrogen peroxide as the photo-Fenton process. A simplified
137 diagram of the overall process is shown in Fig. 1.

138

139 Fig. 1.

140

141 2.3. *Membrane filtration*

142 NF-90 and BW-30 membranes supplied by Dow/Filmtec were evaluated in this investigation on the basis
143 of their distinct molecular weight cut-offs (MWCO) and zeta-potential values at neutral pH (Lopez-
144 Muñoz et al., 2009). These membranes were received as flat sheet samples. According to the
145 manufacturers, the studied membranes are polyamide thin-film composite with a microporous
146 polysulfone supporting layer. Table 2 summarizes their most relevant features. The reverse osmosis
147 membrane (RO), BW-30, is designed to purify water with high biological or organic fouling potential in
148 systems with well-controlled pretreatment. The nanofiltration membrane (NF), NF-90, is widely used for
149 the removal of divalent salts and organic compounds (Nghiem et al, 2007).

150

151 Table 2

152

153 Selected membranes were tested as flat sheet membrane specimens in a commercial SEPA II cross-flow
154 filtration test cell (Osmonics, Minnetonka, MN). The experimental set-up has been previously described
155 elsewhere (Arsuaga et al., 2011). The effective membrane area in the test unit is 139 cm². Prior to each
156 experiment, membranes were soaked in ultrapure water for a minimum of 24 h. During this period

157 ultrapure water was replaced every 4-8 h to remove chemicals used for membrane preservation.
158 Additionally, the membranes were pre-compacted for approximately 1 h at 20 bar until constant flux.

159 In order to explore the separation efficiency of the selected NF/RO membranes, the filtration experiments
160 were carried out in a reconcentration mode, collecting the permeate stream in a external vessel and
161 recirculating the retentate stream to the feed tank up to a volume reduction factor of 10, being defined this
162 factor as the ratio between the initial volume (V_0) and the final retentate volume (V_r). The volume of the
163 initial aqueous solution with the selected pharmaceuticals was 20 L. The first volume pumped from the
164 tank at the beginning of each experiment was left out in order to guarantee the homogeneous content of
165 feed stream (the dead volume of the filtration setup is approximately 1 L). The permeate flux was
166 determined gravimetrically by weighting the mass of permeate stream collected at predetermined time
167 interval (1 min) with an analytical balance. The retention performance of NF-90 and BW-30 membranes
168 was compared in terms of initial and final concentrations of the feed stream at the beginning and the end
169 of the reconcentration experiment. Temperature was controlled at 25 °C. Trans-membrane pressure was
170 fixed at 5.5 bar and 14.8 bar in NF-90 and BW-30, respectively. To reduce membrane fouling and effects
171 due to concentration polarization, a high cross-flow velocity was selected (1.5 ms^{-1}).

172 In order to explore the influence of solute sorption on the performance of tested membranes, preliminary
173 permeation experiments were operated in a recycling mode in which both concentrate and permeate
174 streams were flowed back to the feed tank. Experiments were extended until steady flux and retention
175 values were reached. In all cases, the drop of the pharmaceutical concentrations due to solute adsorption
176 was lower than 5 %. These results are in agreement with recent published studies related to adsorption of
177 organic solutes on the membrane surface and the filtration performance of NF-90 and BW-30 membranes
178 (Sotto et al, 2013).

179 **2.4. Experimental set-up of the photocatalytic oxidation systems**

180 Concentrated effluent rejected by the membrane unit was treated by means of two heterogeneous
181 photocatalytic oxidation processes under UV-Visible light irradiation: i) photocatalytic oxidation
182 (UV/TiO₂) and ii) Fe₂O₃/SBA-15 photo-Fenton (UV/Fe₂O₃/H₂O₂). In both cases, the photocatalytic
183 experiments were carried out in a cylindrical Pyrex batch reactor of 1 L as effective solution volume (.
184 This photo-reactor provides an overture located on the top to submerge the lamp and two additional
185 openings for withdrawing samples and air bubbling if necessary (heterogeneous photocatalysis
186 experiments).

187

188 The irradiation of the reacting solution was performed with an immersed 150 W medium pressure
189 mercury lamp (Heraeus TQ-150) placed inside a jacket. This jacket was used for the circulation of a
190 copper sulphate solution (0.01 M) as a cooling system to prevent overheating of the reaction mixture and
191 to absorb energetic UV irradiation with wavelengths below 320 nm. The lamp was always switched on
192 for 15 min before being fitted into the reactor, in order to achieve a stabilised radiation emission
193 (Martinez et al., 2005).

194 Typically, for photo-catalytic oxidation, 1.0 gL⁻¹ of catalyst (TiO₂, Degussa P25) was added to the
195 pharmaceutical aqueous solution, and 80 mLmin⁻¹ air flow was bubbled in the reacting mixture
196 throughout the overall catalytic experiment. For photo-Fenton oxidation, 0.6 gL⁻¹ of Fe₂O₃/SBA-15
197 catalyst was used and the pH of the reacting mixture was adjusted to ca. 3 with a sulfuric aqueous
198 solution (0.1 M). The photo-Fenton catalyst based on ca. 18 wt% of Fe₂O₃ supported over a mesoporous
199 SBA-15 silica catalyst was prepared according to the procedure reported elsewhere (Martínez et al.,
200 2005). In both catalytic runs (UV/TiO₂ and UV/Fe₂O₃/H₂O₂), the catalysts were maintained in suspension
201 by a magnetic stirrer placed at the bottom of the reactor. In the case of photo-assisted experiments that
202 requires hydrogen peroxide (UV/H₂O₂ and UV/Fe₂O₃/H₂O₂), 0.135 gL⁻¹ of the oxidant was set by addition
203 of aqueous hydrogen peroxide solution (33% p/v) in the concentrated pharmaceutical solution just after
204 the stabilization the radiation emission. The efficiency of all the photoassisted catalytic systems was
205 assessed for periods of treatment of 6 hours taking aliquots from the reactor along the time at fixed
206 intervals.

207

208 2.5 *Characterization of aqueous samples*

209 Prior to characterization, all the samples were filtered through 0.22 µm nylon filters in order to remove
210 the suspended solids. The concentration of pharmaceutical compounds was measured by means of a
211 HPLC chromatograph Varian Prostar apparatus equipped with a Phenomenex Gemini column (150 x 3.0
212 mm) and an array diode detector. A 150 µL volume loop was filled with sample, from which a total
213 volume of 50 µL was injected into the column. A gradient method with 20mM formic acid and
214 acetonitrile mobile phase, starting with a volume ratio of 10:90 and finishing in 100:0 after 45 minutes
215 was employed (total flow rate 0.2 mL/min). UV absorbance at 275 was used for the determination of all
216 the compounds except nicotine, in which the detector was set to 254 nm. All samples were analysed by

217 duplicate. Additionally, standard samples of calibration were periodically analyzed every 10 samples in
218 order to verify the repeatability of the measurements. The variation of the standards along an analysis
219 sequence was always lower than 5%. The quantification limit of this method was set to 0.5 mgL^{-1} for all
220 the pharmaceutical compounds in basis of the standard deviation of the measurements of blank samples
221 multiplied by 15.

222 Total organic carbon (TOC) content of the samples was analyzed using a combustion/non dispersive
223 infrared gas analyzer model Shimadzu TOC-V. Repetitive measurements of both standards and samples
224 of reaction did not exceed 5% difference for the range of the measured TOC concentrations. Hydrogen
225 peroxide concentration in the samples taken off from the photocatalytic runs that the oxidant was
226 measured by iodometric titration, with an error interval confidence of $\pm 15 \text{ mgL}^{-1}$.

227

228 3. Results and discussion

229

230 3.1 *Reconcentration of pharmaceuticals by nanofiltration and reverse osmosis*

231 Fig. 2 shows the retention comparison between NF-90 and BW-30 membranes displayed in terms of
232 initial and final concentrations of experiments in reconcentration mode. As expected, the reverse osmosis
233 BW-30 membrane exhibited systematically, for all solutes, larger retention rates than NF-90 membrane;
234 although the differences are hardly significant. The highest final concentrations were found for 4-AAA
235 and ranitidine in both nanofiltration and reverse osmosis experiments. For the other four solutes (NCT,
236 HCT, SMX and DCF) NF-90 membrane showed a rather similar reconcentration performance, whereas
237 the final reconcentration values were more distinct when the BW-30 membrane was employed.

238

239 Fig. 2.

240

241 Regarding to the molecular weight of PhACs as descriptor of molecular size, the differences of final
242 concentrations of ranitidine (highest value) and nicotine (lowest value) show that steric hindrance is the
243 main factor determining the retention capacity of both membranes. Hydrophobic interaction and electric
244 repulsion between solute species and the membrane surface seem to be of minor importance. However,
245 the comparatively high rejection of 4-AAA for the tested membranes can be attributed to a cooperative
246 effect of two compound characteristics: size and hydrophilic nature. Since 4-AAA molecules remain

247 mainly uncharged at pH 7, electrostatic interaction between solute and the negatively charged surface
248 membrane can be neglected (Nghiem et al, 2007). On the other hand, when comparing the physico-
249 chemical parameters of 4-AAA with the values of the other investigated PhACs of similar molecular
250 weight, its hydrophilic nature is remarkable (Table 1). Consequently, hydrophobic interaction between
251 organic solute and membrane surface to promote the solute transfer through the membrane is less favored
252 for 4-AAA.

253 In order to combine membrane technology with photocatalytic processes processes the NF-90 membrane
254 was selected for the proposal of pharmaceutical reconcentration. The selection of this membrane was
255 based in considerations of time saving (permeability for NF-90 membrane is quite larger) and power
256 saving (BW-30 membrane operates at higher pressure), since the observed differences between them in
257 terms of the retention capacity for the selected compounds were not significant (Fig. 3). For this reason, a
258 more detailed study of the membrane performance was solely carried out for NF-90.

259 Membrane flux performance was studied by observing the permeate flux evolution at constant pressure as
260 a function of time (Fig.3). Significant flux decline is observed during the fouling run. The flux drops
261 steeply around 20 % at the initial stage of the filtration run (first 12 h). After that, the flux decreases
262 slowly during the next 12 h exhibiting a permeate flux decline of 5%. Finally, the permeate flux of NF-90
263 membrane decreases rapidly promoting an additional flux reduction of 13 % after 32 hours of experiment.
264 For the whole interval time studied, the flux reaches no apparent stationary state with equilibrium values.
265 At this point, it can be assumed that the deposition/adsorption of pharmaceuticals on the membrane
266 surface could be the main responsible of the observed flux declines (Nghiem et al, 2007; Sotto et al,
267 2013). Previous studies have suggested that organic deposition onto the membrane surface can destabilize
268 the membrane performance, causing a denser fouling layer with greater hydraulic resistance (Van der
269 Bruggen, 2008). The flux decline observed at the initial stage is probably caused by pore restriction and
270 initial deposition of organics on the membrane surface. The gradual decline exhibited by membrane in the
271 intermediate stage of the filtration process could be associated to the thickening as well as the compaction
272 of the fouling layer. After that, the severe flux drop observed in the membrane performance after 24 h of
273 running could be explained both by pore blocking process or cake layer formation. Pore blocking
274 essentially results in a decrease of the membrane porosity and an increase in membrane resistance to mass
275 transfer. It is caused by bulk phase solutes that are small enough to enter into the membrane pores and

276 deposit on their surface. The solutes that are retained on the membrane surface either attach to the
277 membrane or contribute to cake layer formation (Sotto et al, 2013).

278

279 Fig. 3.

280 The time-dependence of compound concentrations in the rejected flux during the filtration with the NF-90
281 membrane at pH 7 are illustrated in Fig. 4. For all compounds the concentration in the rejected flux
282 increases. The simultaneous solute concentration in the permeate stream remains almost invariable.
283 Hence, it is clearly evident that the feed concentration and the corresponding concentration in the rejected
284 stream should increase as result of decreasing of water feed volume in the reconcentration test.

285

286 Fig. 4.

287

288 Temporal evolution of solute reconcentration displayed in Fig. 4 is in accordance with the values shown
289 in Fig. 2. As previously discussed, steric hindrance is the main physico-chemical effect determining
290 PhAcs rejection, except for 4AAA. Concentration in the rejected stream (concentrate) slowly increases
291 (almost linearly) until an abrupt change is observed. This rapid variation occurs around after 24 h of the
292 filtration run, which is in agreement with the behavior of temporal flux evolution described in the
293 previous Figure 3. For this reason, the concentration increasing at the final stage of operation could be
294 associated to the fouling effect (cake layer formation). On the other hand, during the filtration
295 experiments, the permeate concentration for every pharmaceutical compound was found almost constant
296 for the studied time interval below the detection limit of the analytical procedure (0.5 mgL^{-1}).

297

298 **3.2 Heterogeneous photocatalytic treatments of concentrated stream from nanofiltration** 299 **membrane separation**

300 After 32 hours of NF-90 membrane operation under reconcentration mode, the concentrated solution was
301 treated by two UV-heterogeneous oxidation processes: TiO_2 photocatalysis and $\text{Fe}_2\text{O}_3/\text{SBA-15}$ photo-
302 Fenton.

303

304 *3.2.1. Performance of TiO₂ photocatalysis*

305 Preliminary blank experiments were performed to evaluate the extent of dark adsorption and photolysis
306 on the degradation of the different pharmaceutical compounds. Fig. 5 shows the degradation profiles of
307 each pharmaceutical at the different experimental conditions. As it can be observed for the dark
308 adsorption test, hydrochlorothiazide showed the highest affinity for the TiO₂ particle surface, achieving a
309 50% of adsorption after 6 hours. A 30% and ca. 20% of adsorption was measured for diclofenac and
310 ranitidine, respectively, at the end of treatment, whereas no significant adsorption was observed for the
311 other pharmaceutical compounds.

312 The experiments performed only with UV-Vis irradiation in the absence of catalyst displayed a distinct
313 sensitivity of each pharmaceutical to direct photolysis by UV-Vis irradiation. The concentration of
314 nicotine, hydrochlorothiazide and the 4-AAA, remained almost constant after 6 hours of irradiation. By
315 contrast, diclofenac sodium was degraded around 60% and sulfamethoxazole and ranitidine hydrochloride
316 were 20% degraded after 6 hours. Degradation of the latter pharmaceuticals by direct photolysis has been
317 previously reported in the literature. However, there are some discrepancies in the efficiency of the
318 process that can be justified in terms of the experimental conditions employed in each case, such as the
319 applied intensity and type of UV light and the initial pharmaceutical concentrations. Kim et al. (2009)
320 demonstrated that sulfamethoxazole and diclofenac are photo-sensible to UV irradiation. They found a
321 high removal efficiency (>95%) for both compounds using a low pressure mercury lamp with maximum
322 wavelength at 254 nm. Beltrán et al. (2008) observed a total disappearance of 10⁻⁴ M sulfamethoxazole at
323 40 minutes of reaction using a high pressure mercury lamp with bandwidth in the range 238–579 nm. Our
324 results for sulfamethoxazole photolytic degradation (Fig. 5) are in agreement with those obtained under
325 sun-light irradiation, a rapid decay of 40% of the initial concentration of the pharmaceutical (10 mgL⁻¹)
326 during the first 45 minutes of irradiation, followed by a slowdown of the degradation rate for longer
327 reaction times (Trovó et al., 2009). Degradation of diclofenac by photolysis processes has been previously
328 reported to occur by exposition to a Xe lamp (Méndez-Arriaga et al., 2008) and under solar radiation
329 (Perez-Estrada et al., 2005; Balters et al., 2007) and it is attributed to the tailing over 300 nm of its
330 maximum absorption centred at 273 nm.

331

332 Fig. 5.

333

334 Irradiation of pharmaceutical compounds in the presence of TiO₂ resulted in a remarkable enhancement
335 of the degradation activity as compared to photolysis or adsorption experiments. After 6 hours of reaction,
336 all pharmaceuticals compounds had approximately a 90% of removal (100% in the case of diclofenac
337 sodium), with the exception of nicotine which has demonstrated to be the most refractory compound to
338 the TiO₂ photocatalytic treatment among all pharmaceuticals evaluated. Photocatalytic degradation of
339 diclofenac, ranitidine, sulfamethoxazole and hydrochlorothiazide showed typical first-order kinetics (with
340 initial reaction rates of 1.25, 0.87, 0.63 and 0.57 mgL⁻¹min⁻¹, respectively), whereas the kinetics for 4-
341 AAA and nicotine disappearance are closer to zero-order. It is interesting to note that in the two latter
342 compounds the contribution of both adsorption and photolysis on the overall process was negligible. The
343 faster degradation was found for diclofenac sodium for which >99% removal was achieved within 70 min
344 of irradiation. The pH of the solution along the reactions above 7 ensures that the disappearance of
345 diclofenac cannot be attributed to the pollutant precipitation at acidic conditions as it has been reported in
346 literature (Perez-Estrada et al., 2005). On the other side, the slower degradation rate of nicotine could be
347 related to its scarce affinity for adsorption on TiO₂ (Fig. 5) or to the negative influence of the other
348 pharmaceuticals or by-products present in the reaction mixture.

349 The TOC mineralization was also measured, obtaining ca. 20 % after 6 hours. This result shows that even
350 though the evaluated pharmaceuticals are prone to undergo photocatalytic degradation with TiO₂, they are
351 not easily mineralized. The reaction proceeds through the formation of a variety of by-products which are
352 not completely oxidized to CO₂ and H₂O, at least after 6 hours of operation.

353

354 *3.2.2. Performance of Fe₂O₃/SBA-15 photoFenton*

355

356 The heterogeneous photo-Fenton system based on the application of home-made Fe₂O₃/SBA-15 catalyst
357 and H₂O₂ has been also employed. Similar photocatalytic system was also used for the abatement of
358 pharmaceuticals in surface rivers (Rodriguez-Gil et al., 2010). The photo-Fenton reaction involves the
359 addition of a strong oxidant such as the hydrogen peroxide, the acidification of the reaction medium and a
360 heterogeneous catalyst with remarkable photocatalytic properties (Martinez et al., 2005; Rodriguez-Gil et
361 al., 2010). For those reasons, several blank reactions were carried out in order to establish the influence of

362 those variables in the overall activity of the photo-Fenton system. The results of these experiments have
363 been also included in Fig.6.

364

365 Fig. 6.

366

367 The photolysis of the pharmaceuticals in presence of hydrogen peroxide was firstly evaluated, in
368 comparison with only UV photolysis presented previously in Fig. 5. The hydrogen peroxide hardly affects
369 the results obtained by only UV-Vis irradiation, achieving similar degradation rates in both cases. Only in
370 the case of ranitidine, a higher degradation was observed (from 20% to 85% after 6 hours of
371 reaction). These results seem to be related to a low hydroxyl radical production from hydrogen peroxide
372 photolysis as consequence of the incident UV-Vis irradiation (higher than 320 nm). Acidification of the
373 solution in absence of UV, H₂O₂ and catalyst produced a significant disappearance of diclofenac sodium.
374 The adjustment of the pH of the solution (close to 3) can be responsible of the pollutant precipitation,
375 although not its degradation, as it has been previously mentioned (Perez-Estrada et al., 2005).
376 Additionally, 4-AAA, hydrochlorothiazide and sulfomethoxazole partially disappeared after acidification
377 (ca. 20% of removal in all cases). This fact may be consequence of changes of speciation by pH-
378 dependence instead of effective oxidation and could have some influence in the overall degradation
379 obtained by the photo-Fenton system. The combination of the hydrogen peroxide and acid conditions
380 without UV irradiation and catalyst yielded a remarkable removal of ranitidine. It can be attributed to the
381 oxidizing power of hydrogen peroxide even without activation of UV-Vis irradiation, and it makes sense
382 the results previously shown by the experiment carried out with hydrogen peroxide in presence of UV-Vis
383 irradiation. For the rest of pharmaceutical compounds, the effect of acidification and hydrogen peroxide is
384 not of statistic relevance. An additional experiment was carried out with the catalyst in absence of UV
385 and hydrogen peroxide. Ruling out the effect of the pH in the diclofenac sodium removal, the
386 disappearance of hydrochlorothiazide and sulfomethoxazole (60 and 40 %, respectively) clearly evidences
387 a significant contribution of the adsorption phenomena on the photo-Fenton catalyst. However, this result
388 can be explained in two different ways. On one hand, it can be attested that removal of these compounds
389 can be driven by its adsorption over the photo-Fenton catalysts assuming that the photo-oxidation reaction
390 take place over the catalyst surface. On the second hand, it could be considered that pharmaceutical
391 compounds can be adsorbed instead of degraded, particularly in the case of low disappearance degrees.

392 Regarding the photo-Fenton system, a high efficiency in the degradation of the six pharmaceutical
393 compounds was exhibited, achieving a total degradation of the pharmaceuticals, except for ranitidine and
394 nicotine. Nevertheless, a remarkable degradation of ca. 90% and 85% for ranitidine and nicotine were
395 obtained. The high degradation degree obtaining for the nicotine, the most refractory compound for the
396 TiO_2 heterogeneous catalyst could be related to the influence of the initial pH of the photo-Fenton
397 reaction. As it has been reported in literature, the dominant nicotine specie at the pH of the photo-Fenton
398 experiment (3.0) is diprotonated nicotine, which has shown a higher photodegradation rate with
399 wavelength of 254 nm (Nienow et al., 2009). Nevertheless, an induction period of 100 minutes is
400 observed before starting the degradation process. This period of time is just the necessary to obtain a
401 degradation grade higher than 90 % for the other pharmaceuticals. This result suggests that the induction
402 period for the nicotine can be related to the selective oxidation of the other chemicals rather than the
403 nicotine. It should be pointed out that this fact has been also observed using goethite as heterogeneous
404 Fenton-like catalyst for the treatment of a mixture of different pharmaceutical pollutants (Molina et al.,
405 2012).

406 The degradation profiles of the pharmaceutical compounds are typical of a first-order kinetic with
407 constants of 0.66, 0.62, 0.69 and $1.09 \text{ mgL}^{-1}\text{min}^{-1}$ for RNT, 4-AAA, HCT and SMX, respectively.
408 However, a zero-order kinetic was also obtained for nicotine after the induction period. The faster
409 degradation was obtained for the diclonenac sodium, although the decrease of pH until ca. 3 at the
410 beginning of the photo-Fenton experiment can be responsible of the pollutant precipitation, preventing the
411 degradation of the compound, as it has been previously mentioned. It should be pointed out that the
412 maximum degradation of each compound is obtained after 180 min, and the rest of the treatment is
413 necessary only to ensure a remarkable degradation of the nicotine.

414 The initial hydrogen peroxide dosage is considered a critical variable affecting the effectiveness of the
415 oxidation process. The influence of this variable was studied by different photo-Fenton experiments using
416 other initial hydrogen peroxide concentrations of 0.05, 0.1, 0.2, 0.3 and 0.4 g/L. Results shown that initial
417 oxidant concentration lower than 0.135 g/L (0.05 and 0.1 g/L) yielded a decrease in the overall
418 performance of the photo-Fenton treatment. Concentrations of 0.2 and 0.3 g/L did not show a relevant
419 enhancement and 0.4 g/L even led to the decrease of performance for some of the pharmaceuticals, which
420 is attributed to secondary reactions of scavenging of hydroxyl radicals. Thus, 0.135 g/L of hydrogen
421 peroxide was established as optimum initial oxidant concentration in the range of study.

422 A remarkable TOC mineralization of the pharmaceuticals (ca. 46%) was achieved by the photo-Fenton
423 system after 6 hours, although the presence of remaining oxygenated by-products of less molecular
424 weight seems is still significant. A common problem of these remaining by-products is related to their
425 plausible toxicity. In a previous work, the application of photo-Fenton process for the abatement of a
426 wide variety of pharmaceuticals detected in surface river waters demonstrated the removal of all these
427 compounds with a remarkable reduction of acute phytotoxicity but a remaining chronic toxicity after
428 treatment (Rodriguez Gil et al., 2010). In this work, a more exhaustive investigation of toxicity was not
429 carried, but further studies based on specific bioassays of acute and chronic toxicities should be done in
430 order to asses the overall performance of the photocatalytic processes.

431

432 4. **Conclusions**

433

434 Coupling of membrane separation and heterogeneous photocatalytic oxidation processes is a feasible
435 alternative for the treatment of pharmaceutical contaminated wastewaters. Nanofiltration membrane
436 exhibits better conditions for the integrated system, in terms of time saving and power operation. This
437 membrane allows obtaining a permeate stream free of pharmaceuticals (below 0.5 mgL^{-1}). The resulting
438 concentrate stream was successfully treated by heterogeneous TiO_2 photocatalysis and the $\text{Fe}_2\text{O}_3/\text{SBA-15}$
439 photo-Fenton processes. In both systems, remarkable degradation removals of all six pharmaceuticals
440 were obtained. TiO_2 photocatalysis achieved a lower degradation of nicotine and mineralization of the
441 organic compounds in terms of the TOC reduction. $\text{Fe}_2\text{O}_3/\text{SBA-15}$ photo-Fenton system enhanced the
442 nicotine removal as well as the TOC mineralization degree, although acidification and hydrogen peroxide
443 as extra oxidant were required. This work evidences the potential alternative of coupling
444 membrane/heterogeneous photocatalytic in order to reduce the continuous discharge of non-
445 biodegradable pharmaceutical compounds through the WWTP effluents. This combination would ensure
446 not only the effective separation of pharmaceuticals, but also their degradation by photo-oxidation.
447 Additionally, the used heterogeneous photocatalysts, TiO_2 or $\text{Fe}_2\text{O}_3/\text{SBA-15}$, prevents the contamination
448 of the effluents by the inclusion of the catalyst in the liquid phase.

449

450 **Acknowledgments**

451

452 The authors thank the financial support of the Spanish Government provided through CONSOLIDER
453 INGENIO 2010 program and the Regional Government of Madrid provided through project
454 REMTAVARES and the European Social. Thanks are also given to Genesys Membrane Product, S.L. for
455 its valuable contribution to this work.

456

457

458

459 **REFERENCES**

460

461 Al-Rifai, J., Gabelish, C., Schäfer, A., 2007. Occurrence of pharmaceutically active and nonsteroidal
462 estrogenic compounds in three different wastewater recycling schemes in Australia. *Chemosphere* 69,
463 803-15.

464 Arsuaga, J.M., Sotto, A., López-Muñoz, M.J., Braeken, L., 2011. Influence of type and position of
465 functional groups of phenolic compounds on NF/RO performance. *Journal of Membrane Science* 372 (1-
466 2), 380-386.

467 Baran, W., Sochacka, J., Wardas, W., 2006. Toxicity and biodegradability of sulfonamides and products
468 of their photocatalytic degradation in aqueous solutions, *Chemosphere* 65, 1295-1299.

469 Bartels, P., von Tümpling, Jr.W., 2007. Solar irradiation influence on the decomposition process of
470 diclofenac in surface waters. *Science of the Total Environment* 374, 143-155.

471 Beltran, F. J., Aguinaco, A., Garcia-Araya, J. F., Oropesa A., 2008. Ozone and photocatalytic processes to
472 remove the antibiotic sulfamethoxazole from water. *Water Research* 42, 3799-3808.

473 Boussu, K., Vandecasteele, C., Van der Bruggen, B., 2008. Relation between membrane characteristics
474 and performance in nanofiltration. *Journal of Membrane Science* 310 (1-2) 51-65.

475 Braeken, L., Bettens, B., Boussu, K., Van der Meer, P., Cocquyt, J., Vermant, J., Van der Bruggen, B.,
476 2006. Transport mechanisms of dissolved organic compounds in aqueous solution during nanofiltration.
477 *Journal of Membrane Science* 279 (1-2) 311-319.

478 Clara, M., Strenn, B., Gans, O., Martinez, E., Kreuzinger, N., Kroiss, H., 2005. Removal of selected
479 pharmaceuticals, fragrances and endocrine disrupting compounds in a membrane bioreactor and
480 conventional wastewater treatment plants. *Water Research* 39 (19) 4797-4807.

481 Farre, M., Perez, S., Kantiani, L., Barcelo, D., 2008. Fate and toxicity of emerging pollutants, their
482 metabolites and transformation products in the aquatic environment. *TrAC-Trends in Analytical*
483 *Chemistry* 27, 991-1007.

484 Gómez, M.J., Martínez Bueno, M.J., Lacorte, S., Fernández-Alba, A.R., Agüera, A., 2007. Pilot Surrey
485 monitoring pharmaceuticals and related compounds in a sewage treatment plant located on the
486 Mediterranean coast. *Chemosphere* 66, 993-1002.

487 Gros, M., Petrovic, M., Barceló, D., 2007. Wastewater treatment plants as a pathway for aquatic
488 contamination by pharmaceuticals in the Ebro river basin (northeast Spain). *Environmental Toxicology*
489 *and Chemistry* 26 (8), 1553-1562.

490 Gros, M., Petrovic, M., Ginebreda, A., Barceló, D., 2010. Removal of pharmaceuticals during wastewater
491 treatment and environmental risk assessment using hazard indexes. *Environment International* 36, 15–26.

492 Grzechulska-Damszel, J., Tomaszewska, M., Morawski, A.W., 2009. Integration of photocatalysis with
493 membrane processes for purification of water contaminated with organic dyes. *Desalination* 241, 118-
494 126.

495 Klammerth, N., Rizzo, L., Malato, S., Maldonado, M. I., Agüera, A., Fernández-Alba, A., 2010.
496 Degradation of fifteen emerging contaminants at mg L⁻¹ initial concentrations by mild solar photo-Fenton
497 in MWTP effluents. *Water Research* 44 545-554.

498 Klavarioti, M., Mantzavinos, D., Kassinos, D., 2009. Removal of residual pharmaceuticals from aqueous
499 systems by advanced oxidation processes, *Environment International* 35 402-417.

500 López-Muñoz, M.J., Sotto, A., Arsuaga, J.M., Van der Bruggen, B., 2009. Influence of membrane, solute
501 and solution properties on the retention of phenolic compounds in aqueous solution by
502 nanofiltration membranes. *Separation and Purification Technology* 66 (1) 194-201.

503 Martínez, F., Calleja, G., Melero, J.A., Molina, R., 2005. Heterogeneous photo-Fenton degradation of
504 phenolic aqueous solutions over iron-containing SBA-15 catalyst *Applied Catalysis B: Environmental* 60,
505 181-190.

506 Martínez Bueno, M.J., Aguera, A., Gomez, M.J., Hernando, M.D., Garcia-Reyes, J.F., Fernandez-Alba
507 A.R., 2007. Application of liquid chromatography/quadrupole-linear ion trap mass spectrometry and
508 time-of-flight mass spectrometry to the determination of pharmaceuticals and related contaminants in
509 wastewater. *Analytical Chemistry* 79 (24), 9372-9384.

510 Méndez-Arriaga, F., Esplugas, S., Giménez, J., 2008. Photocatalytic degradation of non-steroidal anti-
511 inflammatory drugs with TiO₂ and simulated solar irradiation. *Water Research* 42, 585-594.

512 Miège, C., Choubert, J. M., Ribeiro, L., Eusèbe, M., Coquery, M., 2009. Fate of pharmaceuticals and
513 personal care products in wastewater treatment plants. Conception of a database and first results.
514 *Environmental Pollution* 157 (5) 1721-1726.

515 Molina, R., Segura, Y., Martinez, F., Melero, J. A., 2012. Immobilization of active and stable goethite
516 coated-films by a dip-coating process and its application for photo-Fenton systems. *Chemical Engineering*
517 *Journal* 203, 212-222.

518 Molinari, R., Pirillo, F., Loddo, V., Palmisano L., 2006. Heterogenous photocatalytic degradation of
519 pharmaceuticals in water using polycrystalline TiO₂ and a nanofiltration membrane reactor. *Catalysis*
520 *Today* 118, 205-213.

521 Mozia S., Morawski A. W., Toyoda M., Tsumura T. Integration of photocatalysis and membrane
522 distillation for removal of mono- and poly-azo dyes from water *Desalination* 250 (2010) 666–672

523 Nghiem, L. D., Schäfer, A. I., Elimelech, M., 2005. Pharmaceutical retention mechanism by
524 nanofiltration membranes. *Environmental Science and Technology* 39 (19) 7698-7705.

525 Nghiem, L. D., Hawkes, S., 2007. Effects of membrane fouling on the nanofiltration of pharmaceutically
526 active compounds (PhACs): Mechanisms and role of membrane pore size *Separation and Purification*
527 *Technology* 57 (1), 176-184.

528 Nienow, A. M., Hua, I., Poyer, I. C., Bezares-Cruz, J. C., Jafvert, C. T., 2009. Multifactorial
529 Analysis of H₂O₂-enhanced photodegradation of nicotine and phosphamidon. *Industrial and Engineering*
530 *Chemistry Research*, 48, 3955-3963.

531 Ozaki, H., Ikejima, N., Shimizu, Y., Fukami, K., Taniguchi, S., Takanami, R., Giri, R. R., Matsui, S.,
532 2008. Rejection of pharmaceuticals and personal care products (PPCPs) and endocrine disrupting

533 chemicals (EDCs) by low pressure reverse osmosis membranes. *Water Science and Technology* 58 (1)
534 73-81.

535 Pérez-Estrada, L., Maldonado, M.I., Gernjak, W., Agüera, A., Fernández-Alba, A.R., Ballesteros, M.M.,
536 Malato, S., 2005. Decomposition of diclofenac by solar driven photocatalysis at pilot plant scale.
537 *Catalysis Today* 101, 219-226.

538 Rodríguez-Gil, J. L., Catala, M., Gonzalez Alonso, S., Romo Maroto R., Valcarcel, Y., Segura, Y.,
539 Molina, R., Melero, J. A., Martinez, F., 2010. Heterogeneous photo-Fenton treatment for the reduction of
540 pharmaceutical contamination in Madrid rivers and ecotoxicological evaluation by a miniaturized fern
541 spores bioassay. *Chemosphere* 80, 381-388.

542 Santos, J.L, Aparicio, I, Alonso, E. 2010. Occurrence and risk assessment of pharmaceutically active
543 compounds in wastewater treatment plants. A case study: Seville city (Spain). *Environmental*
544 *International* 33, 596-601.

545 Shemer, H., Kunukcu, Y. K., Linden, K. G., 2006. Degradation of the pharmaceutical metronidazole via
546 UV, Fenton and photo-Fenton processes. *Chemosphere* 63, 269–276.

547 Simon, A., Nghiem, L. D., Le-Clech, P., Khan, S. J., Drewes, J. E., 2009. Effects of membrane
548 degradation on the removal of pharmaceutically active compounds (PhACs) by NF/RO filtration
549 processes. *Journal of Membrane Science* 340 (1-2) 16-25.

550 Sotto, A., Arsuaga, J.M., Van der Bruggen, B., 2013. Sorption of phenolic compounds on NF/RO
551 membrane surfaces: Influence on membrane performance. *Desalination* 309, 64-73.

552 Trovó, A. G., Nogueira, R.F.P., Agüera, A., Fernández-Alba, A. R., Sirtori, C., Malato, S., 2009.
553 Degradation of sulfamethoxazole in water by solar photo-Fenton. Chemical and toxicological evaluation.
554 *Water Research* 43, 3922-3931.

555 Van der Bruggen, B., Mänttari, M., Nyström, M., 2008. Drawbacks of applying nanofiltration and how to
556 avoid them: A review. *Separation and Purification Technology* 63 (2), 251-263.

557 Verliefde, A.R.D., Heijman, S.G.J., Cornelissen, E.R, Amy, G. L., Van der Bruggen, B., Van Dijk, J. C.,
558 2009. Influence of electrostatic interactions on the rejection with NF and assessment of the removal
559 efficiency during NF/GAC treatment of pharmaceutically active compounds in surface water. *Water*
560 *Research* 41 (15), 3227-3240.

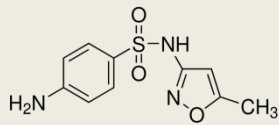
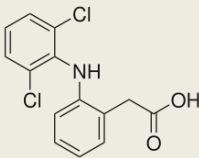
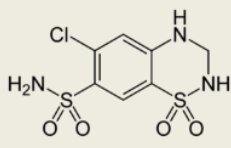
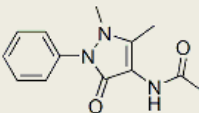
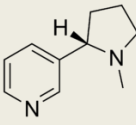
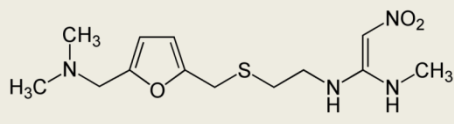
561 Xu, W., Zhang, G., Li, X., Zou, S., Li, P., Hu, Z., Li, J., 2007. Occurrence and elimination of antibiotics
 562 at four sewage treatment plants in the Pearl River Delta (PRD), South China. *Water Research* 41, 4526-
 563 4534.

564 Yang, L., Yu, L. E., Ray, M. B., 2008. Degradation of paracetamol in aqueous solutions by TiO₂
 565 photocatalysis. *Water Res* 42, 3480-3488.

566

567 **Tables**

Table 1. Intrinsic physicochemical properties of selected pharmaceuticals

Compound	Structure	MW(gmol ⁻¹)	logK _{ow}	pK _a
Sulfamethoxazole (SMX)		253.3	0.9	5.8
Diclofenac ^a (DCF)		296.2	4.5	4.1
Hydrochlorothiazide (HCT)		297.7	-0.5	7.9
4-Acetamidoantipyrine (4-AAA)		245.3	-0.1	4.6 ^b
Nicotine (NCT)		162.2	1.1	3.1 ^b
Ranitidine hydrochloride ^c (RNT)		350.9	1.3	8.2 ^b

a Reported data corresponds to pure diclofenac (acid form), although the sodium salt was actually used.

b pK_a of the monoprotonated form

c Hydrochloric acid is not displayed in the chemical structure

568

569

Table 2. Physicochemical properties of selected membranes

	NF-90	BW-30
Manufacturer	Dow/Filmtec	Dow/Filmtec
Classified as	NF	RO
Active layer material	Polyamide	Polyamide
MWCO	200	N.A.
NaCl rejection (%)	90	99
Test pressure (psi)	70	225
pH range	4-11	2-11
Membrane charge (pH 7)	-26.5	-5.2
Pure water permeability [L / m ² day kPa] (25°C)	2.49	0.67
Contact angle(°)	63.2	62

571

572 **Figure Captions**

573 Fig. 1. Scheme of the coupling separation/photocatalytic processes.

574

575 Fig. 2. Comparative of initial and final concentrations for NF-90(A) and BW-30(B)
576 membranes as result of reconcentration experiments from 20 L of feed solution.

577

578 Fig. 3. Temporal evolution of permeate flux for NF-90 membrane during
579 reconcentration experiments.

580

581 Fig. 4. Pharmaceutical concentrations of the rejected flux as a function of filtration time
582 for the NF-90 membrane. Concentrate stream was circulated back to the feed tank
583 during experiments.

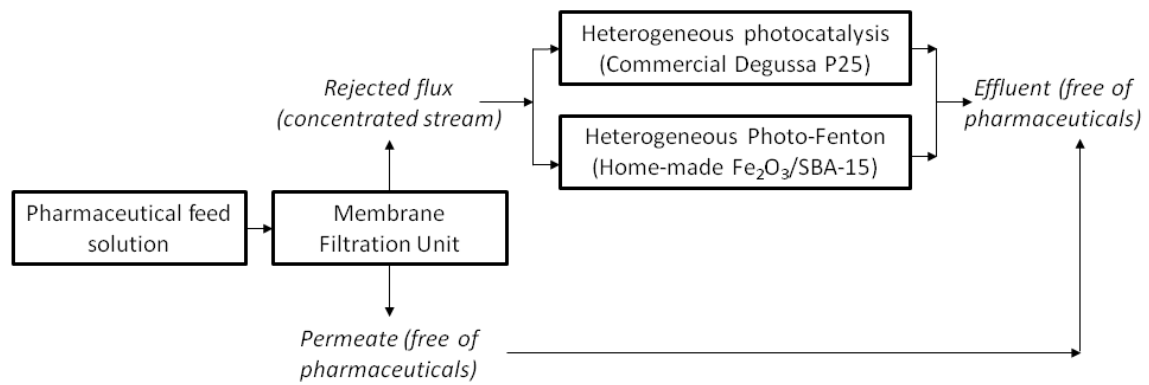
584

585 Fig. 5. Pharmaceutical profiles for the TiO_2 photocatalysis treatment of the rejected flux
586 and blank reactions related. ■ Photo-catalysis with TiO_2 , ▲ Adsorption in absence of
587 UV, ● Photolysis in absence of TiO_2 .

588
589 Fig. 6. Pharmaceutical profiles for $\text{Fe}_2\text{O}_3/\text{SBA-15}$ photo-Fenton treatment of the
590 rejected flux and the blank reactions related: ▽ Photo-Fenton reaction, Δ Photolysis
591 with hydrogen peroxide, ◇ Acidification in absence of UV, H_2O_2 and catalyst, ○
592 Acidification with H_2O_2 in a dark system in absence catalyst, □ Adsorption over the
593 catalyst in absence of UV and H_2O_2 .

594

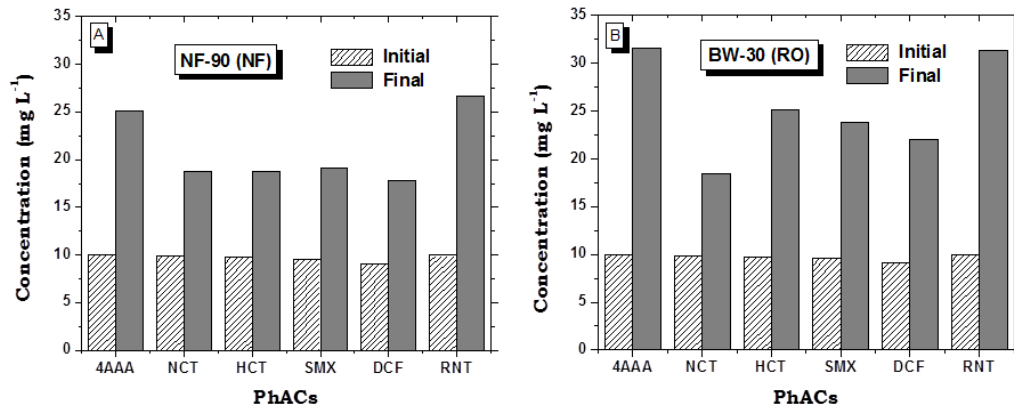
595



596

597 Fig 1.

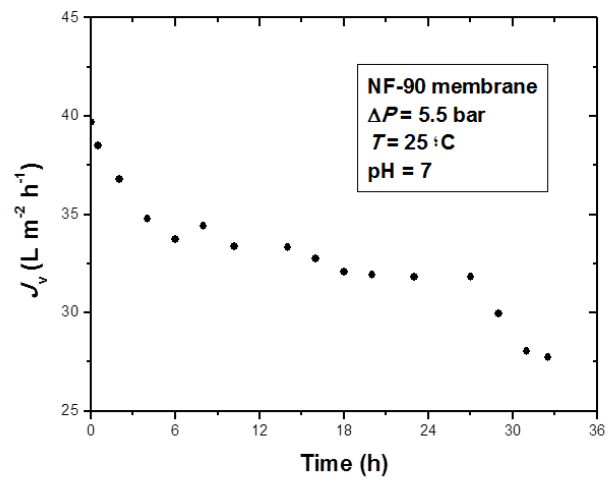
598



599

600 Fig 2.

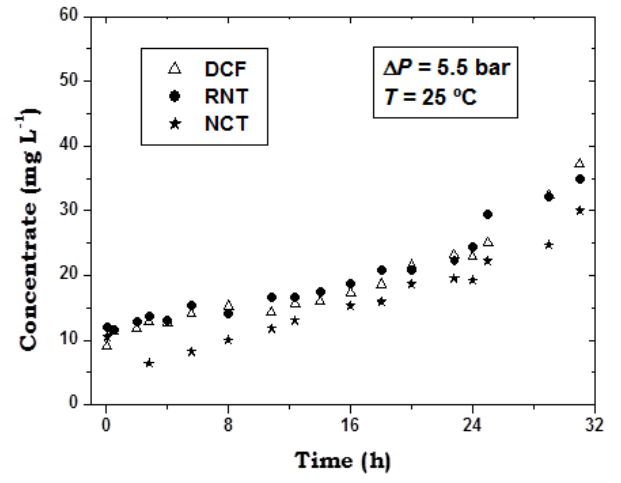
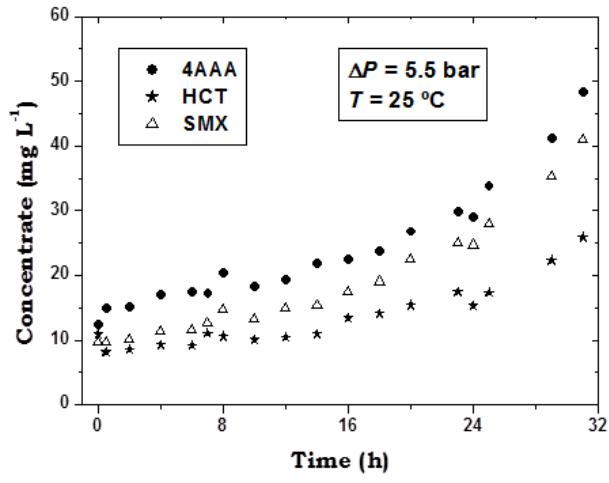
601



602

603 Fig 3.

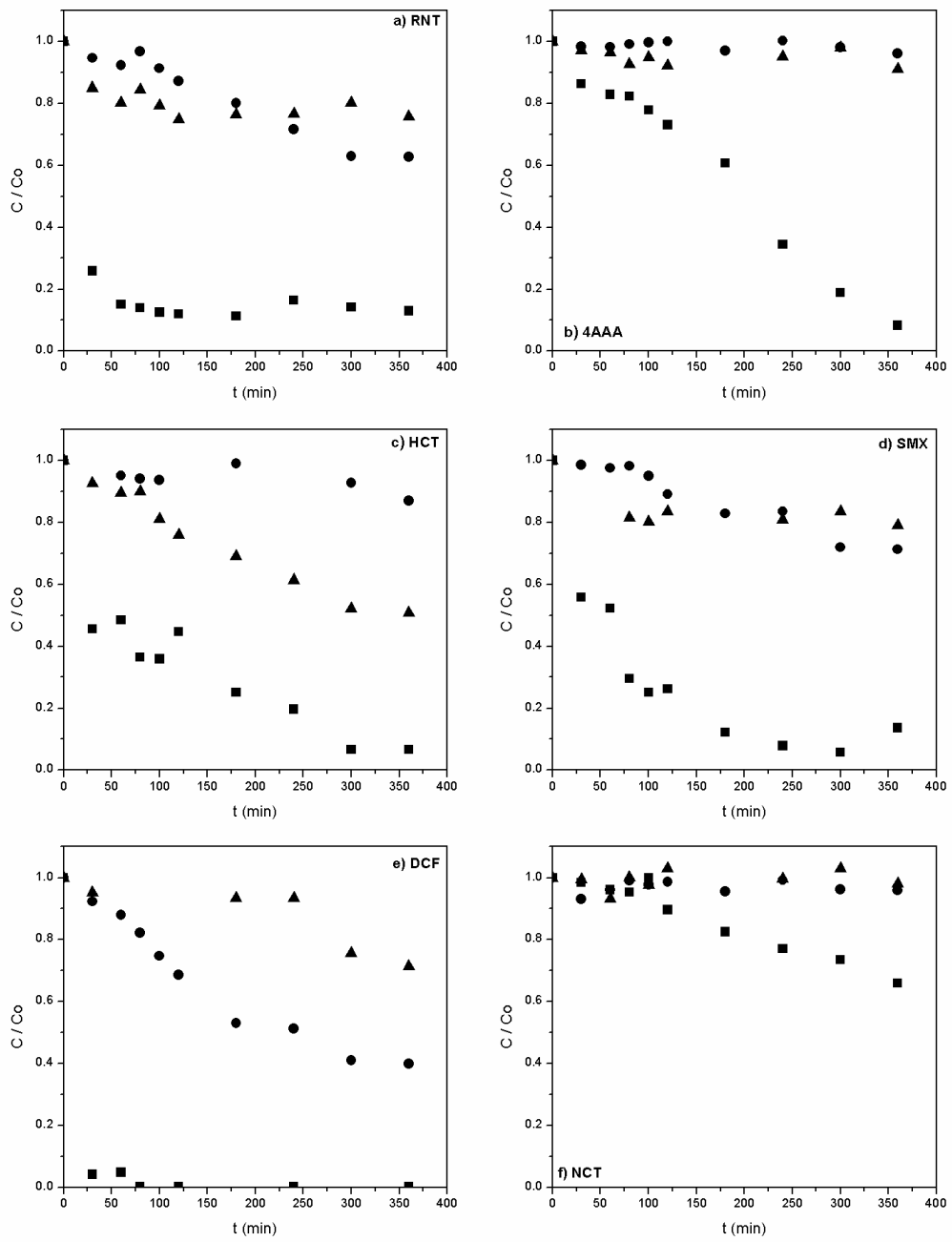
604



605

606 Fig 4.

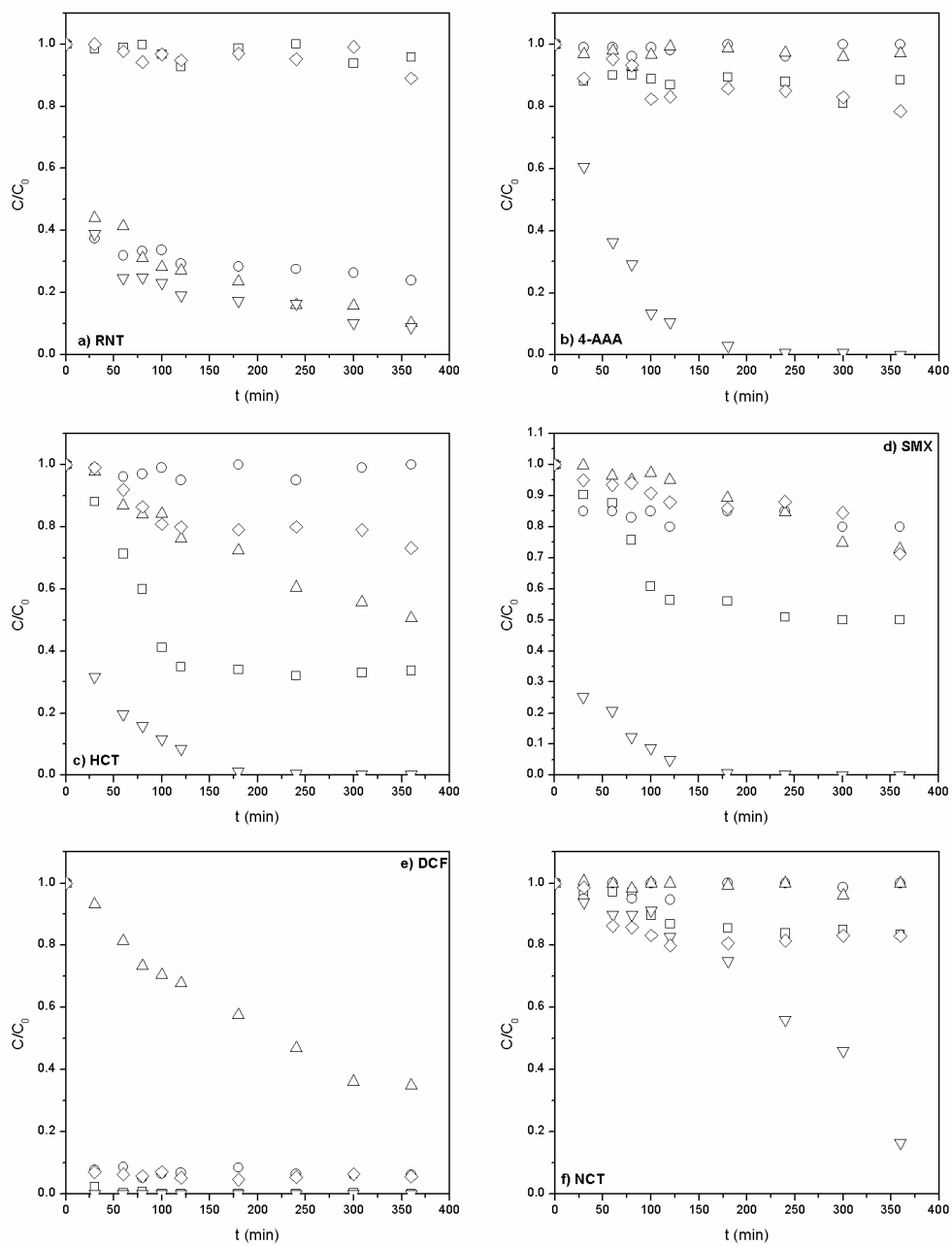
607



608

609 Fig 5.

610



611

612 Fig 6.

613